Chaotic behaviour in a Singular Perturbed System

Ignacio B. Vivancos.[*] Antonmaria A. Minzoni.

FENOMEC
IIMAS-UNAM
Apdo. Postal 20-726. México D.F.

November 30, 2000

Abstract

The aim of this paper is to present a novel type of chaos observed in a four dimensional singularly perturbed system. The chaotic behaviour is described both numerically and analytically. We show the existence of a new type of strange attractor reminiscent of a chaotic behaviour for a fast-slow system. Related to this we demonstrate that there is am invariant attracting region overlapping the jump manifolds of the fast system. This canonical problem was identified to be a coupled problem of two Hopf bifurcations with the fast jump process. We derive a geometric model where we can rigorously show the existence of chaotic orbits.

Keywords: Singular Perturbations, Chaos, 3D attractors.

---

[*] Present address: Lab.Sis.Din, Orense 32, Madrid 28020, Spain.

1 Introduction

Most mathematical analyses of qualitative properties of singularly perturbed systems done so far deal with local studies of phenomena occuring in system equations of low dimensions, see Guckhenheimer [4] for a nice survey on this topic. Our goal in this work is to extend the local analyses and show how interesting global features can appear in four dimensional singularly perturbed systems. One of the main characteristics of singular systems is the fact that they possess different time scales. As a consequence, two dynamically different manifolds appear: a slow manifold where the system varies slowly and a fast manifold generally of lower dimension. Bifurcations in the family of vector fields induce transitions of trajectories from the neighbourhood of one family of attractors to another on the fast time scale. To our knowledge, little is known about systems presenting many transition orbits between these attractors. We do not pretend in this work to make a rigourous analysis of such transitions but rather to exhibit global properties and, in particular, the existence of high dimensional strange attractors.

In this paper we concentrate our efforts on both the analytical and numeric studies of the following singularly perturbed system:

$$\begin{aligned}
\dot{x}_1 &= x_1(\lambda + ax_1^2 + bx_2^2 + cx_3^2) + p_1 x_2 x_3 u \\
\dot{x}_2 &= x_2(\lambda + ax_2^2 + bx_3^2 + cx_1^2) + p_1 x_1 x_3 u \\
\dot{x}_3 &= x_3(\lambda + ax_3^2 + bx_1^2 + cx_2^2) + p_1 x_1 x_2 u \\
\varepsilon \dot{u} &= u(\mu - u^2 + p_2(x_1^2 + x_2^2 + x_3^2)) + p_3 x_1 x_2 x_3,
\end{aligned} \tag{1.1}$$

λ, μ and ε ($1 >> \varepsilon \geq 0$) will be fixed while p_1, p_2, p_3 denote parameters. The first motivation for the study of such system equations comes from a model of planar convection undertaken by Busse and Heikes [1] in 1980. Their mathematical model was intented to mimic the instability (Kuppers-Lortz instability) observed for convective rolls in a rotating layer leading to a three dimensional system of ODEs for the amplitudes (x_1, x_2, x_3) of the velocity field:

$$\begin{aligned}
\dot{x}_1 &= x_1(\lambda + ax_1^2 + bx_2^2 + cx_3^2) \\
\dot{x}_2 &= x_2(\lambda + ax_2^2 + bx_3^2 + cx_1^2) \\
\dot{x}_3 &= x_3(\lambda + ax_3^2 + bx_1^2 + cx_2^2),
\end{aligned} \tag{1.2}$$

.

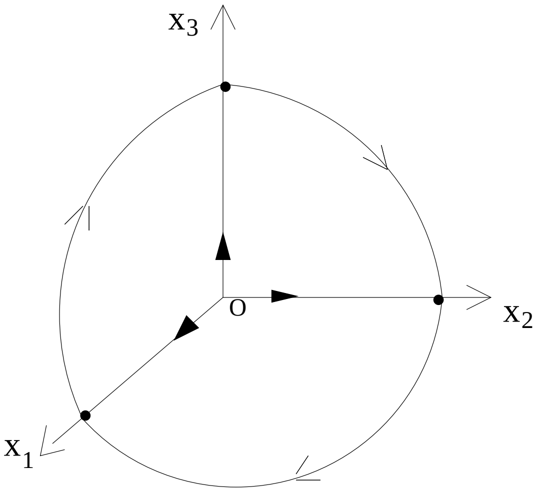

Figure 1: The heteroclinic cycle in $\mathbf{R}^3$ of Guckenheimer and Holmes

By rescaling (x_1, x_2, x_3) and time we can fix

$$\lambda = 1 \quad \text{and} \quad a + b + c = -1.$$

Later on Guckenheimer and Holmes [5] showed the existence of a structurally and asymptotically stable heteroclinic cycle in these equations provided that the coefficients a, b and c satisfy the conditions

$$|a + b + c| = 1 \qquad c < a < b < 0 \quad \text{and} \qquad 2a > b + c. \tag{1.3}$$

This heteroclinic cycle consists of six equilibrium points of saddle type, each lying in the coordinate axes connected by trajectories in the coordinates planes which are invariant by the flow which correspond to fixed point subspaces for the symmetry group $\Gamma = \mathbf{T} \oplus \mathbf{Z}_2$. Here $\mathbf{T}$ acts as a cyclic permutation and $\mathbf{Z}_2$ acts as a reflection. Roughly speaking, we have six equilibrium points each lying in the coordinate axes that are connected by trajectories in the invariant planes $x_i = 0, i = 1, 2, 3$ guaranteed by the Poincaré Bendixon Theorem (see Figure 1).

Starting from system equations (1.2) we will focus our efforts on the study of intermittent chaotic dynamics in the singularly perturbed model (1.1). More specifically, we will study what is called a transverse perturbation of the heteroclinic cycle existing in system (1.2) and in our case, this perturbation will lead us to a singular system as ε is a small parameter. The transverse perturbation consists of adding a fourth equation to the system (1.2) for a dynamic in a direction orthogonal to the original invariant coordinate planes. These kinds of perturbed systems have been studied by several authors within the context of symmetric dynamical systems. Their approach relies heavily on the equivariant bifurcation theory and symmetry group techniques (see Sandstede and Scheel [9], Melbourne and Krupa [6]).

In this paper we will consider a singular transverse perturbation and, for our purposes the symmetry considerations will play a minor role. At first the variable u was meant to mimic the dynamics of a magnetic instability resulting from a convective state described by equations (1.2). The scale for the magnetic mode u arises from the time scale of approach to the limit cycle of the fast dynamics in the velocity variables $x_i, i = 1, 2, 3$. This model failed to be representative of the dynamo effect because of the symmetries of the equation in u. Since the magnetic field should respect the symmetry $u \mapsto -u$ only even powers of u are allowed. This unfortunatelly does not exhibit rich dynamical behaviour for this u variable. Still the work presented here is aimed to gain some insight into what kind of dynamics one can expect when breaking heteroclinic cycles in $\mathbf{R}^3$ that were forced by symmetry. The global behaviour of the perturbed system (1.1) can be very complicated as we will show in the next section despite the apparently simple form of the equation for the u variable. The terms in this equation have the following justification: $\mu < 0$ since we require asymptotic stability, p_1, p_2, p_3 can be of any sign with $p_3 \neq 0$ since the quantity $x_1x_2x_3$ plays a fundamental role as we will show later. The parameter p_1 is responsible for breaking the original heteroclinic connections. Finally the equation for the variable u respects some symmetry properties, notably $(x_1, x_2, x_3, u) \mapsto (-x_1, -x_2, -x_3, -u)$ which simplifies the bifurcation analysis.

As it will become apparent from numerical simulations, chaotic orbits appear in the fourth dimensional system with a reminiscent behaviour inherited from the three dimensional heteroclinic cycle of the system (1.2). More specifically, we observe that these chaotic orbits will exhibit long residing times when passing close to the old equilibria followed by faster movements along the connecting orbits. As a result of the perturbation of such cycle, a new attractor forms in $\mathbf{R}^4$ whose structure presents many stricking novelties. We will show that a 3D strange attractor seems to exist whose structure ressembles the structure of a 2D tent map. This invariant chaotic set is composed by a Cantor-like union of leaves and on each leaf the behaviour is the same one as for the tent map.

The mechanism for the creation of such an object is identified as the result of coupling two Hopf bifurcations in the slow manifolds with a fast jump process transverse to those manifolds. A more detailed analysis shows us that the creation of chaos comes from the situation where the slow manifolds loose normal hyperbolicity and present knees. The structure of these manifolds is inherited from the original heteroclinic connections. The drop points where the orbits jump from one slow manifold to another happen to be far enough from the Hopf equilibria. The geometric situation can be described as a 3-dimensional figure $\mathcal{S}$ whose geometry is the result of adding the new transverse direction to the original 1-dimensional heteroclinic connection.

The layout of the paper is as follows: in Section (2) we present the numerical simulations that induced us to search for chaos. Section (3) is devoted to a bifurcation analysis that allows us to present a geometric model in Section (4). In the singular limit case, $\varepsilon = 0$, we can solve u as a (bi-valuated) function of the slow variables x_1, x_2, x_3 and obtain a 3-dimensional system of equations. It will be assumed that there exists a very strong contracting direction transverse to the slow manifolds that allows us to reduce the study of the dynamics to a two dimensional system of equations. The $\mathcal{C}^1$-approximation theory developed by Mischenko *et al.* [7] will be used for the case $\varepsilon \neq 0$. The proof of the existence of chaos is tackled in Section (5) followed by Section (6) where we rigourously show that there exists at least an invariant curve where the dynamics are conjugated to those of a tent (or hump) map.

Questions as to whether the strange attractor is a suspension or a product of a simple object with a known 2D attractor that arises, for instance, in planar diffeomorphisms remain to be answered.

2 Numerical simulations

The system 1.1 has been numerically integrated using a Runge-Kutta scheme of order 7-8 with adjustable step. The typical phase portrait for an orbit is shown in Figure (2), where we have fixed $a = -0.2,\ b = -0.1,\ c = -0.7$. Without loss of generality these values will remain fixed for the following. Numerical simulations of such system present the following features: typical orbits approach the original heteroclinic connections but do not asymtote to it. After a number of revolutions in the neighborhood of the heteroclinic orbit, say in the first octant, they jump to another octant and repeat the process in a random fashion. At this stage, the chaotic behaviour consists on the unpredictability of the time spent in each octant and the way these octants are visited by the orbit. These erratic excursions depend on the sign and amplitude of the term $p_3 x_1 x_2 x_3$.

Sensitive dependence on initial conditions has been observed in the computer; close initial conditions diverge into completely different trajectories. Besides these erratic excursions, the jumps between the octants for the x_i variables are accompanied by fast reversals of the sign of the variable u. The duration of the epochs will be shown to be also chaotic (see Figure 3).

Figure 4 shows a two dimensional projection of the Poincaré section $u = 0$ for the system (1.1). This three dimensional object ressembles a ribbon with a width that is folded at an angle and ressembles the image of a tent. Most likely this strange attractor is composed as an union of infinitely many one-dimensional tents glued together in a transverse direction. Topologically this object could be the product of an interval together with a tent map. The dynamics along the tent maps are easily proved to be chaotic and the novelty of this new type of strange attractor comes from the fact that its width looks like an interval that could itself be a Cantor set.

Another numerical evidence for the presence of chaos is the existence of positive Lyapunov exponents that are consistent with the existence of a strange attractor. Starting from an infinitesimal four dimensional sphere of initial conditions this sphere deforms into a four dimensional ellipsoid due to the locally deforming nature of the flow. Then the $i_t h$ dimensional Lyapunov exponent is defined in terms of the length of the ellipsoidal principal axes $a_i(t)$. The effective computation of the Lyapunov exponents has been done for different values of the parameters p_i starting from 10 different points chosen equally spaced on a circumference of radius 0.01 around the origin. Then we computed the most positive exponent L_1 up to n=30 000 iterations:

$$L_1 = max_i L_i = \lim_{t \to \infty} Log_2 \frac{a_i(t)}{a_i(0)}$$

The table below presents some parameter values where L_1 is representative. The fixed values are $\mu = -0.05$ and $\varepsilon = 0.01$.

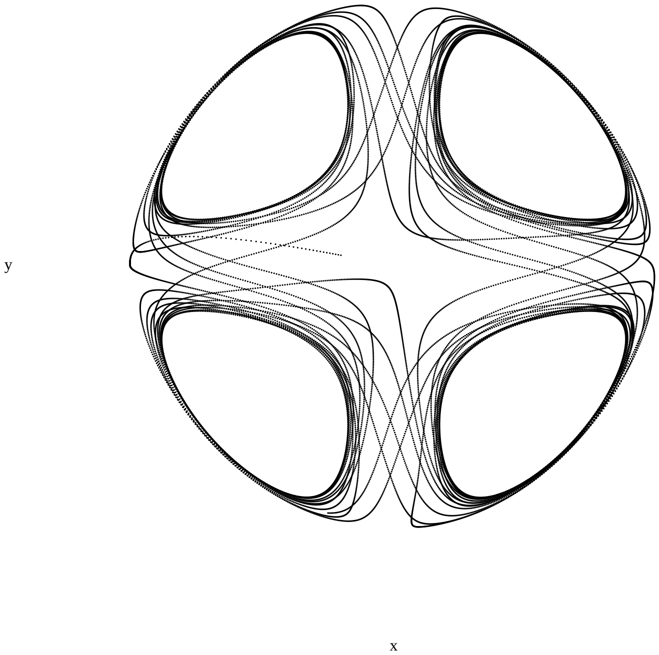

Figure 2: Phase portrait in the x_1, x_2 space for $\mu = -0.05$, $p_1 = -0.07$, $p_2 = 0.5$, $p_3 = 0.8$ and $\varepsilon = 0.01$.

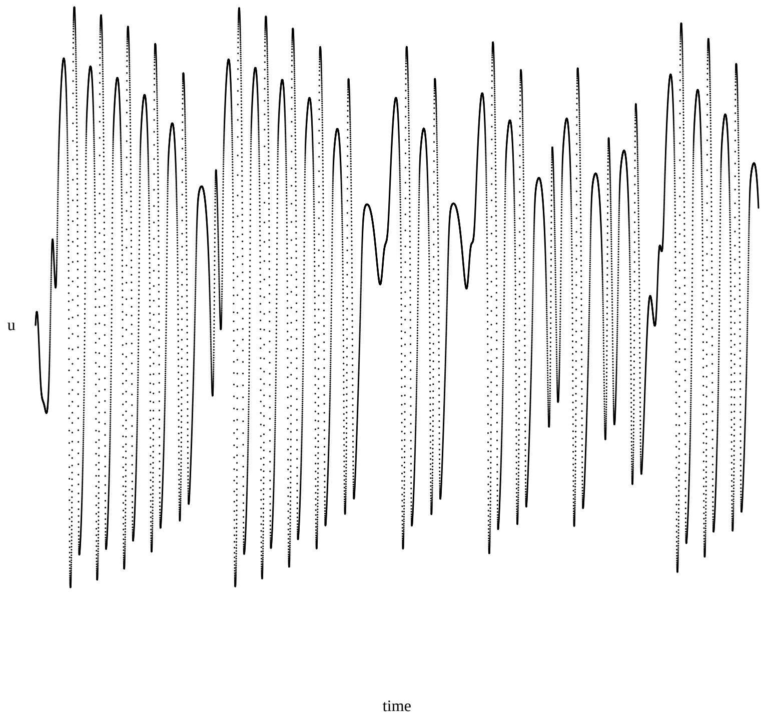

Figure 3: Chaotic behaviour for the u variable.

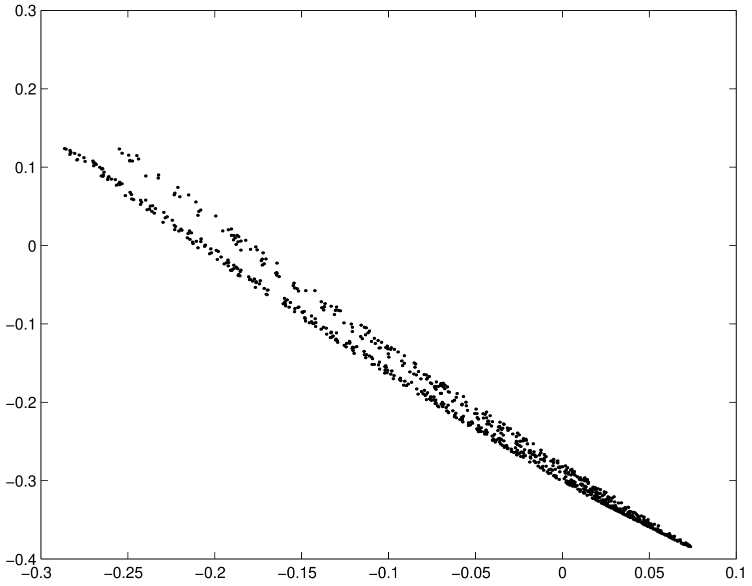

Figure 4: 2D projection of a 3D Poincare section $u = 0$ for the same parameter values as in Figure 2

Parameter values	Lyapunov Exponent
$p_1 = 0.53$ $p_2 = 0.1$ $p_3 = -1.6$	L_1=0.017
$p_1 = 0.23$ $p_2 = -0.2$ $p_3 = -1.6$	L_1=0.34
$p_1 = 0.33$ $p_2 = -0.1$ $p_3 = -1.5$	L_1=0.72
$p_1 = 0.73$ $p_2 = 0.3$ $p_3 = -1.1$	L_1=0.69
$p_1 = 1.03$ $p_2 = 0.6$ $p_3 = -0.8$	L_1=4.45

3 Bifurcation analysis

In order to understand the change in the orbit structure of the flow (1.1) one can restrict attention to a small neighbourhood of those parameter values for which there is a non hyperbolic equilibrium point. The numerical simulations induce us to study the dynamics with the use of fast slow techniques. In fact, we will show that there are slow manifolds that loose normal hyperbolicity. As the parameters are varied, bifurcations take place in which the real part of the eigenvalues associated to the behaviour normal to the invariant planes cross zero. The corresponding invariant manifolds are the core of a chaotic invariant set.

3.1 The bifurcated equilibrium points

Proposition 3.1 *The non trivial equilibria for the system (1.1) are as follows :*

1. *If* $u = 0$, *then* $X^{\pm} = (\pm\sqrt{-\frac{1}{a}}, 0, 0, 0)$, $Y^{\pm} = (0, \pm\sqrt{-\frac{1}{a}}, 0, 0)$ $Z\pm = (0, 0, \pm\sqrt{-\frac{1}{a}}, 0)$ *and* $(\pm 1, \pm 1, \pm 1, 0)$.
2. *If* $u \neq 0$, *and if* $\exists\ x_i = 0, i = 1, 2, 3$ *then* $X_u^{\pm} = (\pm\sqrt{a}, 0, 0, \pm\sqrt{-\mu + \frac{p_2}{a}})$, $Y_u^{\pm} = (0, \pm\sqrt{-\frac{1}{a}}, 0, \pm\sqrt{-\mu + \frac{p_2}{a}})$, $Z_u^{\pm} = (0, 0, \pm\sqrt{-\frac{1}{a}}, \pm\sqrt{-\mu + \frac{p_2}{a}})$.
3. *If* $u \neq 0$ *and* $x_1 x_2 x_3 \neq 0$ *then* $U_i^{\pm} = (x^*, \pm x^*, \pm x^*, u^*)$, $i = 1, \ldots, 4$ u^* *being solution of the cubic polynomial* $u^3 - (3p_2 {x^*}^2 + \mu)u - p_3 {x^*}^3 = 0$, *and* x^* *is given by* $x^* = \frac{1}{2}(p_1 u^* \pm \sqrt{p_1^2 {u^*}^2 + 4})$.

Proposition 3.2 *Type 1 and type 2 equilibria are stable. A Hopf bifurcation occurs at type 3 equilibria* $U_i^{\pm}$ *located on the diagonal axes* $x_1 = \pm x_2 = \pm x_3$ *(see Figure 5).*

Remark that due to the symmetries of the system

$$\begin{aligned}(x_1, x_2, x_3, u) &\mapsto (x_2, x_3, x_1, u)\\(x_1, x_2, x_3, u) &\mapsto (-x_1, x_2, x_3, u)\\(x_1, x_2, x_3, u) &\mapsto (-x_1, -x_2, -x_3, -u),\end{aligned}$$

we can do all the bifurcation analysis in one octant. We will compute the eigenvalues only at the first octant since the others are obtained by cyclic permutation.

Proof

1. The equilibria $X^{\pm}, Y^{\pm}, Z^{\pm}$ are saddles and $(\pm 1, \pm 1, \pm 1, 0)$ are sinks.
2. At the equilibrium X_u^+ the eigenvalues are

   $$\lambda_1 = -2;\ \lambda_2 =; -2(\mu + p_2\frac{1}{|a|})\ \lambda_{3,4} = \frac{1}{2}\Big(2 - (b+c)x^2 \pm \Delta^{1/2}\Big)$$

   where $\Delta = (b-c)^2x^4 + 4p_1^2x^2u^2$ is always positive. Hence all these eigenvalues are real if $p_1 \neq -\frac{a^2-bc}{\mu a+p_2}$.
3. Type $U_i^{\pm}$ equilibria must satisfy the equation :

   $$(x_1^2 - x_2^2) + a(x_1^4 - x_2^4) + bx_2^2(x_1^2 - x_3^2) + cx_1^2(x_3^2 - x_2^2) = 0$$

   whose solutions are $x_1 = \pm x_2 + \pm x_3 = x^*$. This value x^* is given by $x^* = 1/2(p_1u^* \pm \sqrt{p_1^2u^{*2} + 4}$ where u^* is a root of $u^3 - (3p_2x^{*2} + \mu)u - p_3x^{*3} = 0$. The eigenvalues are

   $$\lambda_{1,2} = 1 - p_1u^*x^* + (\pm\sqrt{3}(b-c)i - 3a)x^{*^2}$$

   and $\lambda_{3,4}$ the roots of the polynomial

   $$X^2 + (3(p_2 - 1)x^{*^2} + 3u^{*^2} - 2p_1x^*u^* - \mu - 1)X + 3(3p_2 - p_1p_3)x^{*^4}$$
   $$+3(\mu + p_2)x^{*^2} - 3x^{*^2}u^{*^2} + 2p_1\mu x^*u^* - 6p_1x^*u^{*^3} - 3u^{*^2} + \mu = 0.$$

   Hence there exists an open set of parameter values such that $\mathcal{R}e(\lambda_{3,4}) = 0$.

∎

3.2 The boundness of the attractor

Proposition 3.3 *Consider the vector field X given by system (1.1) with* $\varepsilon = 1$. *Under conditions (1.3) there exists an open set of parameter values such that the closed spherical shell*

$$\mathcal{D} \ = \ \{K \leq x_1^2 + x_2^2 + x_3^2 + u^2 \leq R\}$$

where $R = 3x^{*^2} + u^{*^2}$ *(*x^**,*u^* *as in Proposition (3.1)) attracts all trajectories.*

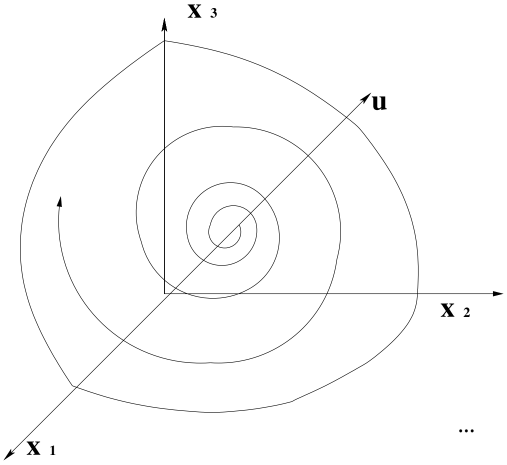

Figure 5: The unstable equilibrium U_1^+.

The closed, simply connected region $\mathcal{D} \subset \mathbf{R}^4$ is such that the vector field is directed everywhere inwards on the boundary. Thus $\mathcal{D}$ contains an attracting set

$$\mathcal{A} = \cap_{t \geq 0} \Phi_t(\mathcal{D})$$

where $\Phi_t(.)$ denotes the flow generated by the system (1.1).

Proof

Take $L(x_1, x_2, x_3, u) = x_1^2 + x_2^2 + x_3^2 + u^2 - R$, then

$$\begin{array}{rcl}
\frac{1}{2}(\nabla.L)\ .\ X & = & a(x_1^4 + x_2^4 + x_3^4) + (b+c)(x_1^2x_2^2 + x_1^2x_3^2 + x_2^2x_3^2) + (x_1^2 + x_2^2 + x_3^2) \\
 & + & (3p_1 + p_3)x_1x_2x_3u + \mu u^2 - u^4 + p_2u^2(x_1^2 + x_2^2 + x_3^2) \\
 & \leq & a(x_1^4 + x_2^4 + x_3^4 + u^4) + (x_1^2 + x_2^2 + x_3^2 + u^2) + (b+c)(x_1^2x_2^2 + x_1^2x_3^2 \\
 & + & x_2^2x_3^2) + \dfrac{(3p_1 + p_3)}{4}(x_1^4 + x_2^4 + x_3^4 + u^4) + p_2u^2(x_1^2 + x_2^2 + x_3^2) \\
 & \leq & (a + \dfrac{(3p_1 + p_3)}{4})(x_1^4 + x_2^4 + x_3^4 + u^4) + (x_1^2 + x_2^2 + x_3^2 + u^2) \\
 & + & p_2(x_1^2x_2^2 + x_1^2x_3^2 + x_2^2x_3^2 + x_1^2u^2 + x_2^2u^2 + x_3^2u^2) \\
 & \leq & \dfrac{1}{3}(a + p_2 + \dfrac{1}{4}(3p_1 + p_3))(x_1^2 + x_2^2 + x_3^2 + u^2)^2 + (x_1^2 + x_2^2 + x_3^2 + u^2)
\end{array}$$

$$\leq \quad (L+R)[(\frac{1}{3}(a+p_2+\frac{1}{4}(3p_1+p_3))(L+R)+1].$$

Take $(a+p_2+\frac{1}{4}(3p_1+p_3)) \leq 0$, and $K^{-1} = -\frac{1}{3}(a+p_2+\frac{1}{4}(3p_1+p_3))$. It follows that L increases along non-zero trajectories while they lie inside $\mathcal{D}$ with the exception of the equilibria $(x^*, \pm x^*, \pm x^*, u^*)$. When $L \geq R$, L decreases along trajectories (see Figure 6).

∎

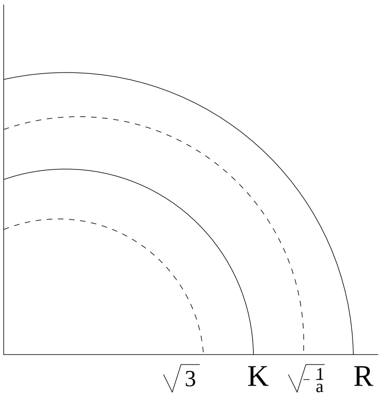

Figure 6: Transversal section of the spherical shell.

As it is shown in Proposition (3.3) there is an attracting spherical region containing the heteroclinic cycle for $u \neq 0$. Notice that the dynamics in the variable u are always bounded. In fact, let us denote

$$P(x_1,x_2,x_3,u) \;=\; u(\mu - u^2 + p_2(x_1^2+x_2^2+x_3^2)) + p_3x_1x_2x_3.$$

Observe that when $x_1x_2x_3 = 0$, the roots $\tilde{r}_{1,2} = \pm\sqrt{\mu + p_2(x_1^2+x_2^2+x_3^2)}$ and $\tilde{r}_3 = 0$, are such that $D_uP(u,x_1,x_2,x_3) = \mu + p_2(x_1^2+x_2^2+x_3^2) > 0$ at $\tilde{r}_3$ while at $\tilde{r}_1$ and $\tilde{r}_2$ $D_uP(u,x_1,x_2,x_3) = -2(\mu + p_2(x_1^2+x_2^2+x_3^2)) < 0$. By structural stability of these hyperbolic points, that is, as long as the roots do not collapse, and except at the particular point where the hyper plane $x_1x_2x_3$ is tangent to $D_uP(x_1,x_2,x_3,u) = 0$, we can conclude that for $x_1x_2x_3 \neq 0$ the variable u also remains bounded and two stable roots r_1, r_2 persist.

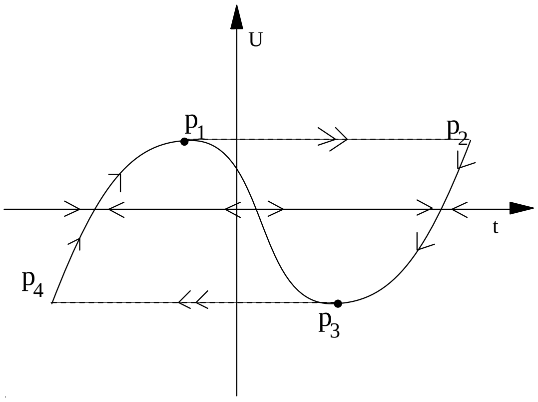

Figure 7: The cubic polynomial $P(x_1, x_2, x_3, u)$

4 The geometric model

The numerical simulations presented in Section 2 can now be interpreted as follows: starting at any point in the region $\mathcal{D}$ the trajectory spirals around a type $U_i^{\pm}$ equilibrium and approaches one of the old heteroclinic connections. The time scale for u arises from the time scake of approach to the limit cycle. During that period the variable u moves in a 'fast manifold' and oscillates i.e changes sign rapidly. After that, the orbit passes close to an equilibrium point of type 2 and joins a ‘slow manifold‘ where u slowly increases (decreases) until a critical value that corresponds to a point $p_{1,2,3,4}$ in the upper (lower) branch, depending on the value and sign of the quantity $x_1x_2x_3$ (see Figure 7)

By replacing the variable u by either one of the stable roots $r_{1,3}$ of the polynomial $P(x_1, x_2, x_3, u)$ we obtain for $\varepsilon = 0$ a singular system having solutions which exhibit jumps. Let $u_1 = \varphi_1(x_1, x_2, x_3), u_2 = \varphi_2(x_1, x_2, x_3)$ denote the slow manifolds. Substituting the expression for u into the system we obtain:

$$\begin{cases} \dot{x}_1 = x_1(1 + ax_1^2 + bx_2^2 + cx_3^2) + p_1x_2x_3\varphi_i(x_1, x_2, x_3) \\ \dot{x}_2 = x_2(1 + ax_2^2 + bx_3^2 + cx_1^2) + p_1x_1x_3\varphi_i(x_1, x_2, x_3) \\ \dot{x}_3 = x_3(1 + ax_3^2 + bx_1^2 + cx_2^2) + p_1x_1x_2\varphi_i(x_1, x_2, x_3) \qquad i = 1, 2. \end{cases}$$

By virtue of the center manifold theorem for a Hopf bifurcation, we can write the system above into the normal form

$$\begin{pmatrix} \dot{x} \\ \dot{y} \\ \dot{z} \end{pmatrix} = \begin{pmatrix} \alpha(u) & -\beta(u) & 0 \\ -\beta(u) & \alpha(u) & 0 \\ 0 & 0 & \varrho(u) \end{pmatrix} \begin{pmatrix} x \\ y \\ z \end{pmatrix} + \begin{pmatrix} P(x,y,z;p_1) \\ Q(x,y,z;p_1) \\ R(x,y,z;p_1) \end{pmatrix},$$

where P, Q, R are nonlinear terms which vanish at the equilibria. The parameter p_1 controls the local bifurcation assumed to occur at $\varrho(u_c) = 0$ and be supercritical; for $u \neq u_c$ $\varrho(u)$ is taken to be negative and $\alpha(u)$ positive with $|\alpha(u)| > |\varrho(u)|$ and with the jump conditions imposed on the surfaces of double roots. The perturbation theory for singularly perturbed systems guarantees the persistence of singular orbits when $\varepsilon \neq 0$. However it is difficult to obtain explicit information from the Poincaré map due to the 3-dimensional nature of the system.

In our case since $\varrho(u_{1,2})$ are negative we have a strong contracting direction and we can use the center manifold reduction for both systems and reduce the study to a 2-dimensional system which takes the form

$$\begin{pmatrix} \dot{\tilde{x}} \\ \dot{\tilde{y}} \end{pmatrix} = \begin{pmatrix} \alpha(u) & -\beta(u) \\ -\beta(u) & \alpha(u) \end{pmatrix} \begin{pmatrix} \dot{\tilde{x}} \\ \dot{\tilde{y}} \end{pmatrix} + \tilde{Q} \begin{pmatrix} \dot{\tilde{x}} \\ \dot{\tilde{y}} \end{pmatrix},$$

together with the matching conditions on the center manifold $\tilde{z} = \Psi(\tilde{x}, \tilde{y})$ along curves where $\varphi_1(\tilde{x}, \tilde{y}) = \varphi_2(\tilde{x}, \tilde{y})$. An appropriate set of parameter values exists such that the center manifold where the solution lies intersects with the drop point. Clearly there are many model equations which have singular limit as the proposed structure. We will later show that a singular system that couples two Hopf bifurcations at different points can have an associated Poincaré map which is non monotone and even chaotic. In what follows we denote $\overline{X} = (x_1, x_2)$. The model system takes the form

$$\begin{cases} \dot{\overline{X}} = F(\overline{X}, u) \\ \varepsilon \dot{u} = (u - r_1(\overline{X}))(u - r_2(\overline{X}))(u - r_3(\overline{X})). \end{cases}$$

The singular system is thus

$$\dot{\overline{X}} = F(\ \overline{X}, \varphi_{1,2}(\overline{X})\ ),$$

with the continuity condition along the curves of double roots $r_{1,2}(\overline{X}) = r_3(\overline{X})$.

It follows from Proposition (3.2) that on the r_1 and r_2-manifolds the flow undergoes a Hopf bifurcation at the points $u = u_1$ and $u = u_2$. Moreover, there is an attracting center manifold at both points $u_{1,2}$ where the bifurcation takes place.

Initial conditions starting near the r_1-manifold are attracted to the shell. The center manifold where the solution lies intersects with the drop point on the r_1-manifold. Then the solution jumps to the r_2 branch and this process is repeated. As the parameter regime is changed the only amplitude effect is the possibility of jumping between different octants in the r_1 or r_2-manifold.

There is another situation when the parameters are such that the attracting shell never intersects with the drop point of the r_1, r_2-manifold. In such case the motion is constrained either to r_1 or to r_2. The Hopf bifurcated orbit can be continued to finite amplitude, and all solutions tend asymptotically to this periodic orbit. This case has been studied as a perturbation of the heteroclinic cycle for the simple case of a quadratic equation for u, where there is only one stable root (see [2]). We also remark that systems presenting a "switch" have been studied numerically by Deng [3] in the singular limit case. However the question of coupled Hopf bifurcations is not addressed. Also the problem of persistence of the chaotic orbits for $\varepsilon \neq 0$ is not studied analytically.

5 The Poincaré maps

Based on the geometric model described in the previous section our goal now is to obtain an explicit expression for the corresponding Poincaré map. The geometric construction will be as follows: starting from any point x_l^1 in a slow manifold close to an unstable (saddle-focus) equilibrium of type 3 the orbit spirals in the unstable manifold until it reaches the drop section in a point x_l^2. Then it instantaneously jumps to another slow manifold. This is the situation observed in figure 2 when the orbit switches from one octant to another. In this process u varies very fast. Once in the new slow manifold the orbit will join at a certain point x_u^2 the unstable manifold corresponding to a new unstable equilibrium of type 3 . Again it will spiral outwards before hitting a new drop section at a point x_u^1 (see Figure 8). This process is repeated infinitely many times. In the same figure we have sketched the transverse direction which is assumed to be strongly attracting.

The Poincaré map we construct is the composition of two different maps ϕ^i and ψ^i. The auxiliary maps ϕ^i are defined by the flow connecting two break points. This map, for $\varepsilon > 0$ is a singular perturbation from the case $\varepsilon = 0$ where ϕ_0 is just a projection. We could take a more general connecting diffeomorphism but it would not introduce any qualitative changes in the dynamics we are interested. The second type maps ψ^i are defined by the flow near the equilibria type 3 and away from the

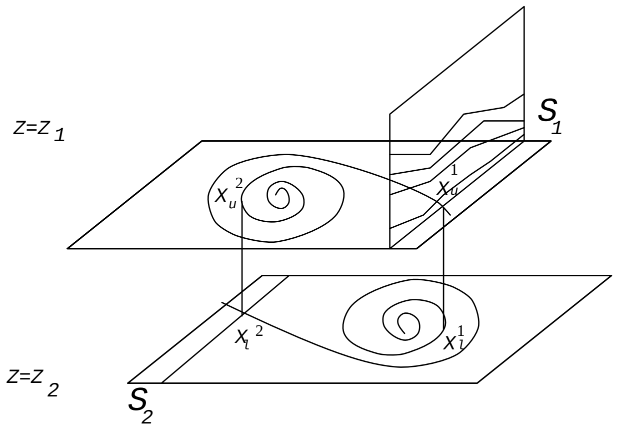

Figure 8: The geometric construction.

break section.

The Poincaré map when $\varepsilon = 0$

We place two planar surfaces $\Sigma_i, i = 0, 1$; each one in a neighborhood of a saddle-focus equilibrium point of type 3 and transverse to the corresponding unstable manifold :

$$\begin{array}{c} \Sigma_1 = \{(x, y, z) \ ; \quad 0 < \delta < y, z = z_1\} \\ \Sigma_2 = \{(x, y, z) \ ; \quad 0 < \delta < y, z = z_2\}. \end{array}$$

Next we define the secants

$$\begin{array}{rcl} S_1 & = & \{(x, y, z) \in \Sigma_1, x = 0\} \\ S_2 & = & \{(x, y, z) \in \Sigma_2, x = A = const\}. \end{array}$$

We shall construct the one dimensional Poincaré map $F_0 : S_1 \to S_1$ as the composition of the maps $\psi^i : \Sigma_i \to S_i \quad i = 1, 2$ and $\phi^1 : S_0 \to \Sigma_1$, $\phi^2 : S_1 \to \Sigma_0$, that is

$$F_0 = \psi_0^1 \circ \phi_0^1 \circ \psi_0^2 \circ \phi_0^2$$

where

$$\psi_0^i(x, y) = \begin{pmatrix} xe^{\mu_i(u)t} \cos \omega_i(u)t + ye^{\mu_i(u)t} \sin \omega_i(u)t \\ xe^{\mu_i(u)t} \sin \omega_i(u)t - ye^{\mu_i(u)t} \cos \omega_i(u)t \end{pmatrix}.$$

Here $\omega_i(u)$ denotes the frequency of the oscillation given by the imaginary part of the eigenvalues which depends continuously on u. We will take for simplicity

$$\phi_0^1(x,y) = (x, y+c), \quad \text{and}$$

$$\phi_0^2(x,y) = (x,y).$$

Here $c > 0$ denotes the offset of the equilibria. From now on we drop the dependence on u. We will make the generic hypothesis that follow:

> *Hypothesis 1* : The drop point is far enough from the saddle-focus equilibrium i.e the offset distance c is large.
>
> *Hypothesis 2* : There exists a set of parameter values such that $\mu_1 > \mu_2 > 0$ and $\omega_2 \simeq \omega_1$.

A direct computation yields the equations:

$$\begin{cases} 0 = ((y+c)e^{\mu_2 t^*} \sin\omega_2 t^*)e^{\mu_1 t}\cos\omega_1 t - ((y+c)e^{\mu_2 t^*}\cos\omega_2 t^*)e^{\mu_1 t}\sin\omega_1 t \\ y = ((y+c)e^{\mu_2 t^*} \sin\omega_2 t^*)e^{\mu_1 t}\sin\omega_1 t + ((y+c)e^{\mu_2 t^*}\cos\omega_2 t^*)e^{\mu_1 t}\cos\omega_1 t \end{cases}$$

where t^* is given by the jump condition $A = (y+c)e^{\mu_2 t^*}\sin\omega_2 t^*$. Assume $\sin\omega_2 t^* \simeq 1$, then $t^* = \frac{1}{\mu_2}\ln(\frac{A}{y+c})$. Hence the total time flight is given by

$$t = \frac{\omega_2}{\omega_1}t^* = \frac{\omega_2}{\omega_1}\frac{1}{\mu_2}\ln(\frac{A}{y+c}).$$

After simplifications the approximated Poincaré map reads:

$$F_0(y) = A^{(1-k)}(y+c)^k\cos(\omega\ln(\frac{y+c}{A}))$$

where

$$k = \frac{\mu_1}{\mu_2}\frac{\omega_2}{\omega_1} > 0 \quad \text{and} \quad \omega = 2\frac{\omega_2}{\mu_2}\ .$$

Taking $\hat{y} + c = \frac{y+c}{A}$ and dropping the hat the final expression yields:

$$F_0(y) = A(y+c)^k\cos(\omega\ln(y+c)).$$

Proposition 5.1 *:*

Let $\Lambda = \{p \in \Sigma_1 \cup \Sigma_2 \; : \; F_0^n(p) \in \Sigma_1 \cup \Sigma_2$ *for each* $n \in \mathbf{N}\}$ *that is,* Λ *is the maximal invariant set of the map* F_0 *restricted to* $\Sigma_1 \cup \Sigma_2$*. Then*

1. Λ *is a Cantor set.*
2. $Per(F_0 \mid_\Lambda)$ *are dense in* Λ*.*
3. F_0 *is transitive on* Λ*.*

Proof :

The zeroes of $F_0(y)$ are $y_0^m = e^{\frac{\pi}{\omega}(1/2+m)} - c$, $m \in N$. Without loss of generality we can restrict our analysis to the interval $\mathcal{I}_0 = [\ y_0^0\ ,\ y_0^1\ ] = [e^{\frac{\pi}{2\omega}} - c, e^{\frac{3\pi}{2\omega}} - c]$.

Now compute

$$\begin{aligned} F_0(y)' &= A(y+c)^{k-1}(k\cos(\omega\ln(y+c)) - \omega\sin(\omega\ln(y+c))) \\ &= A(y+c)^{k-1}\sqrt{k^2+\omega^2}\cos(\omega\ln(y+c)+\theta) \end{aligned}$$

where $\theta = \arctan\frac{\omega}{k} = \arctan(2\frac{\omega_1}{\mu_1})$, now $F_0(y^*)' = 0 \Rightarrow y^* = e^{3\frac{\pi}{2\omega} - \frac{\theta}{\omega}} - c$. Because $\frac{\pi}{2} > \theta > 0$, $y^* \in \mathcal{I}$ is the unique point in $\mathcal{I}_0$ where the derivative vanishes. Hence $F_0(y)$ is strictly monotone increasing on the interval $[e^{\frac{\pi}{2\omega}} - c, y^*[$ and strictly monotone decreasing on the interval $]y^*, e^{\frac{3\pi}{2\omega}} - c]$.

Next compute that

$$|F_0(y^*)| = Ae^{\frac{k}{\omega}(\frac{3\pi}{2} - \theta)}\ |\sin\theta|$$

we claim that $|F_0(y^*)| > L$ where $L = e^{\frac{\pi}{2\omega}}(e^\pi - 1)$ denotes the length of the interval $\mathcal{I}_0$. First notice that $Ae^{\frac{k}{\omega}(3\frac{\pi}{2} - \theta)}\ |\sin\theta| > Ae^{\frac{k}{\omega}\frac{\pi}{2}}\ |\sin\theta|$, hence we need to show that $Ae^{\frac{k}{\omega}\frac{\pi}{2}}\ |\sin\theta|\ >\ e^{\frac{\pi}{2\omega}}(e^\pi - 1)$, that is $Ae^k\ |\sin\theta|\ >\ (e^\pi - 1)$. Replacing terms this means that

$$\frac{A}{\sqrt{1 + (\frac{\mu_1}{2w_1})^2}} > e^{-k}(e^\pi - 1). \tag{5.4}$$

Thanks to *Hypothesis 2* this inequality will be satisfied as long as $A > e^\pi\sqrt{1 + (\frac{\mu_1}{2w_1})^2}$.

Now, there exists two points $\bar{p}_i, i = 1,2$ satisfying $F_0(\bar{p}_i) = e^{\frac{\pi}{2\omega}}(e^\pi - 1)$. Let us denote $\mathcal{I}_1 = [e^{\frac{\pi}{2\omega}} - c, \bar{p_1}]$ and $\mathcal{I}_2 = [\bar{p_2}, e^{\frac{3\pi}{2\omega}} - c]$. Finally let $\mathcal{I} = \cup_{i=1,2}\mathcal{I}_i$. By construction we have $\mathcal{I} \subset F_0(\mathcal{I}_i)$ $i = 1,2$ for all $y \in \mathcal{I} \cap F_0^{-1}(\mathcal{I})$.

Lemma 5.2 *Under hypothesis H(1)-H(2), there exists a real number* $m \geq 1$*, such that* $|F_0(y)'| > m$ *for all* $y \in \mathcal{I} \bigcap F_0^{-1}(\mathcal{I})$*.*

Proof :

$$F_0(y)'' = A\sqrt{k^2+\omega^2}\sqrt{(k-1)^2+\omega^2}(y+c)^{k-2}\cos(\omega ln(y+c)+\theta+\theta^{'}).$$

Here $\theta^{'} = \arctan\frac{w}{k-1}$. The unique point $y^{**} \in \mathcal{I}_0$ satisfying $F_0(y^{**})'' = 0$ is $y^{**} = e^{\frac{1}{\omega}(\frac{3\pi}{2}-\theta-\theta^{'})} - c$, because $\frac{\pi}{2} > \theta^{'} > 0$. Moreover y^{**} does not lie in the interval $\mathcal{I}\bigcap F_0^{-1}(\mathcal{I})$. Clearly y^{**} does not belong to $\mathcal{I}_2$. We also have $y^{**} > p_1$ since $F_0(y^{**}) > F_0(\bar{p_1}) = e^{\frac{\pi}{2\omega}}(e^{\pi}-1)$. To see this, remark first that for $\omega_1 \simeq \omega_2$ and $\mu_1 << \mu_2$ we have $\theta+\theta' = \arctan\frac{4}{\mu_1}$. Also replacing terms $\sin(\theta+\theta') > \sin(\theta)$ as long as $\omega_1 < 2$ which is in the range parameter given by *Hypothesis 2*. Whence $F_0(y^{**}) = Ae^{\frac{k}{\omega}(\frac{3\pi}{2\omega}-\theta-\theta^{'})}\sin(\theta+\theta^{'}) > Ae^{\frac{k}{\omega}(\frac{3\pi}{2\omega}-\theta)}\sin(\theta)$ and by the last inequality $Ae^{\frac{k}{\omega}(\frac{3\pi}{2\omega}-\theta)}\sin(\theta) > e^{\frac{\pi}{2\omega}}(e^{\pi}-1)$. Hence y^{**} is a maximum with $F_0(y)'' > 0$ in $\mathcal{I}_1$ and $F_0(y)'' < 0$ in $\mathcal{I}_2$. The minimum of $|F_0(y)'|$ for $y \in \mathcal{I}_1$ is hence given by $|F_0(y_0^0)'|$ and by $|F_0(y_0^1)'|$ for $y \in \mathcal{I}_2$. It suffices to see that

$$|F_0(y_0^0)'| = A\sqrt{k^2+\omega^2}e^{\frac{\pi}{2\omega}(k-1)}\sin(\theta) > \sqrt{k^2+\omega^2}(e^{\pi}-1) \ > \ 1,$$

using inequality (5.4) and the fact that $k = \frac{\mu_1\omega_2}{\mu_2\omega_1}$ with $\frac{\mu_1}{\mu_2} > 1$ and $\frac{\omega_2}{\omega_1} \simeq 1$. Finally

$$|F_0(y_0^1)'| = A\sqrt{k^2+\omega^2}e^{\frac{3\pi}{2\omega}(k-1)}\sin(\theta) > |F_0(y_0^0)'| > 1.$$

This ends the proof of the lemma.

∎

We are now under the required conditions to conclude that $\Lambda = \bigcap_{n=0}^{\infty} F_0^{-n}(\mathcal{I})$ is a Cantor set (see for instance Robinson [8]). Moreover, define $\mathcal{F}_k : \Lambda \longmapsto \mathbf{S_2}$ (the symbol space on 2 symbols) by $\mathcal{F}_k(y) = t$ where $F_0^n(y) \in \mathcal{I}_{tn}$ then $\mathcal{F}_k$ is a topological conjugacy from F_0 on Λ to the shifting operator on $\mathbf{S_2}$. Finally we can conclude that F_0 is chaotic on Λ, that is $Per(F_0 \mid_\Lambda)$ are dense in Λ and F_0 is transitive on Λ.

∎

It is important to remark that the non monotonicity of the map comes from the spiral structure of the orbit. Hence even if the curve of double roots is not a straight line the same construction will exhibit a non monotone map. Finally the height of the hump is not controlled by the distance between the critical points and the jumping size. It follows that the non monotonicity remains if the curve of double roots is uniformly bounded away from the critical points. We can conclude that the Poincaré map for $\varepsilon = 0$ is conjugated to a hump map and possesses chaotic orbits.

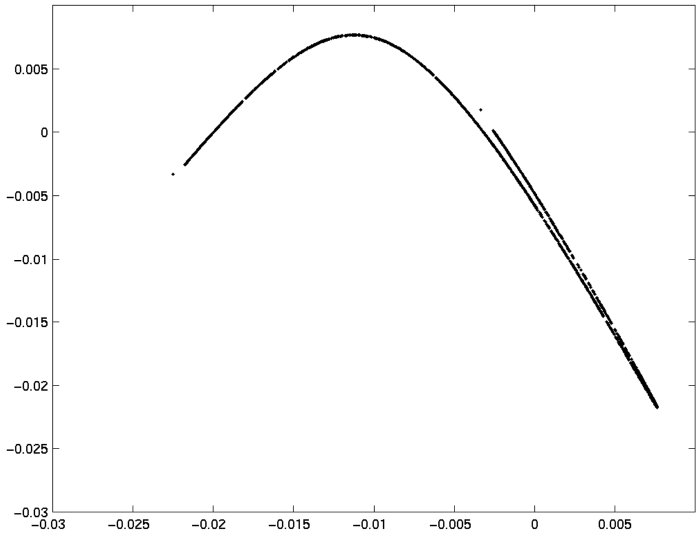

Figure 9: The y_n versus y_{n+1} Ruelle plot as x crosses $x = 0$ from below. The parameter values are : $p_1 = 1.8, p_2 = 0.04, p_3 = 6.5, \mu = -0.005$ and $\varepsilon = 0.01$.

6 Existence of an invariant curve

So far we have demonstrate that the sytem (1.1) possesses chaotic orbits when $\varepsilon = 0$. It is clear from the expression of the Poincaré map $F_0(.)$ that this map is topologically conjugated to the well known hump map. Figure 9 was numerically obtained as the Ruelle plot of either one of the variables $y = x_1, x_2$ or x_3 and agrees with the dynamics of the map $F_0(.)$.

This last section is devoted to the proof that for $\varepsilon \neq 0$ there exists an invariant curve. This curve lives in the three dimensional object presented in Figure 4 and is part of the skeleton of a much more complicated strange attractor. Starting from the Poincaré map derived in the previous section, we can obtain the corresponding Poincaré map for $\varepsilon \neq 0$. The basic tool for this study is the $\mathcal{C}^1$-approximation theory developed by Mischenko *et al.* [7] concerning the Poincaré maps for singularly perturbed systems. It is shown in [7] that one can choose a plane in the space $(\overline{X}, u)$ which is transverse to the flow with coordinate s along the stable manifold, say $u = \varphi_1(\overline{X})$ and coordinate t along the transverse manifold. We have the following theorem:

Theorem 6.1 ([7])
The Poincaré map is given by

$$\mathcal{H}(s,t)=\left\{\begin{array}{l} s\rightarrow F_\varepsilon(s,t)=F_0(s)+\varepsilon^{2/3}\ \tilde{F}_\varepsilon(s,t)\\ t\rightarrow e^{-1/\varepsilon}G_\varepsilon(s,t). \end{array}\right.$$

The maps $F_\varepsilon, G_\varepsilon$ are continuously differentiable with respect s,t and their derivatives are uniformly bounded with respect to ε in the $\mathcal{C}^1$-metric.

The first coordinate is the map for the singular system perturbed by the map of the jump points which is of order $\mathcal{O}(\varepsilon^{2/3})$ due to the scaling of the time in this region. The exponential contraction in the second coordinate is due to the exponential attractive character of the manifolds $u=\varphi_{1,2}(\overline{X})$. We believe that this map possesses dense orbits but were unable to prove it rigorously. Instead we will show the persistence of an invariant curve which is sufficiently smooth and can be expressed in the form $t=\gamma(s)$. On this curve the map takes the form

$$s\rightarrow F_0(s)+\varepsilon^{2/3}F_\varepsilon(s,\gamma(s)).$$

The usual perturbation arguments show the existence of dense orbits (chaotic) for initial conditions on this invariant curve provided the map $F_0(s)$ has the appropriate hump-like shape.

Consider the rectangle $\mathcal{R}=\mathcal{I}_s\times\mathcal{I}_t$. For the following we reparametrize $\mathcal{I}_s=[0,1]$ and $\mathcal{I}_t=[-t_0,t_0]$. Let us denote the disk $\gamma_0=t_0^*\times\mathcal{I}_s,\ t_0^*\in\mathcal{I}_t$. Clearly this straight line is mapped inside the rectangle $\mathcal{R}$ since $\mathcal{H}$ strongly contracts in the vertical direction. This line is then mapped into a curve which folds producing two disjoint curves γ_1^1, γ_1^2 that intersect the original rectangle.

Theorem 6.2 *Consider the successive iterates of a chosen initial curve γ_0 intersection the rectangle $\mathcal{R}$:*

$$\mathcal{R}\cap\mathcal{H}(\gamma_0)=\gamma_1^1\cup\gamma_1^2,\quad \cdots \quad ,\mathcal{R}\cap\mathcal{H}(\gamma_n^{\sigma_n}(s))=\gamma_{n+1}^{\sigma_{n+1}}(s_1)\cup\gamma_{n+1}^{\sigma_{n+1}+1},$$

where $\sigma_n=\underbrace{(\cdots,i_j,\cdots)}_{n}, i_j=1,2$ then, for each σ_n there exists a unique function $t=\gamma_n^{\sigma_n}(s)$ lying on $\mathcal{R}$ which is invariant under the map $\mathcal{H}$.

Take a curve $t=\gamma_0(s)$, its image under $\mathcal{H}$ noted $\gamma_1(s)$ is determined by the functional equation:

$$G(s,\gamma_0(s))=\gamma_1\circ(F(s,\gamma_0(s)). \tag{6.5}$$

Lemma 6.3 *:*

Assume $\gamma_0(s)$ is a $\mathcal{C}^r$ ($r \geq 3$) curve with $|\gamma_0^{'}(s)| \leq \kappa$ where κ is a small positive constant, then $\gamma_1^{'}(s)$ is also $\mathcal{C}^r$ and obeys $|\gamma_1^{'}(s)| \leq \kappa$ for $s \in \mathcal{I}$.

Proof We will denote $G_{s,t}$ and $F_{s,t}$ the partial derivative with respect to the variables s, t. $M_{\{\}}$ and $N_{\{\}}$ will denote constants.

Clearly γ_1 is differentiable since $|F_s| > 1$ for $s \in \mathcal{I}$ and hence $F(s, \gamma_0(s))$ is invertible in this interval. Let us denote $s_1 = F(\gamma_0(s)) + \varepsilon^{2/3}\widetilde{F}(s, \gamma_0(s))$. Differentiating (6.5) gives

$$G_s + \gamma_0^{'}(s)G_t = \gamma_1^{'}(s_1)(F_s + \gamma_0^{'}(s)F_t),$$

hence

$$\gamma_1^{'}(s_1) \ = \ \frac{G_s + \gamma_0^{'}(s)G_t}{F_s + \gamma_0^{'}(s)F_t} \tag{6.6}$$

We estimate first the denominator of this expression. For $s \in \mathcal{I}$ we have $|F_s| > \alpha > 1$ by lemma (5.2) of Section 5 and by lemma (6.3) $|F_t| < M_F$, hence $|F_s + \gamma_0^{'}(s)F_t| > 1 + \kappa M_t > 1$. We also know from lemma (5.2) that there exists some constants $M_{G_s} < 1, M_{G_t} < 1$ such that $|G_s| < M_{G_s}$ and $|G_t| < M_{G_t}$, hence the numerator $|G_s + \gamma_0^{'}(s)G_t| < M_{G_s} + \kappa M_{G_t} < \kappa M_{G_t}$. Combining the estimates for the numerator and the denominator we have:

$$\frac{|G_s + \gamma_0^{'}(s)G_t|}{|F_s + \gamma_0^{'}(s)F_t|} \ < \ \kappa M_{G_t} < \kappa \ .$$

The same argument is iterated to prove $\mathcal{C}^3$-regularity.

∎

We can now proceed to the proof of the Theorem. We will denote $|.|_r$ the $\mathcal{C}^r$ norm. When omitted subscript, $|.|$ means the $\mathcal{C}^0$ norm. Let $\gamma_0(s)$ and $\tilde{\gamma}_0(s)$ be two curves which have the properties being in $\mathcal{R}$ and obeying $\gamma_0^{'}(s), \tilde{\gamma}_0^{'}(s) < \kappa$, then their iterates $\gamma_n^{\sigma_n}(s), \tilde{\gamma}_n^{\sigma_n}(s)$ will also have these properties by lemma (6.3). We prove now that for $s \in \mathcal{I}$, the map $\gamma_n^{\sigma_n}(s) \rightarrow \gamma_{n+1}^{\sigma_{n+1}}(s_1)$ is a contraction in $\mathcal{C}^3$. We only reproduce the details of the proof for the first derivative:

$$|\gamma_{n+1}^{\sigma_{n+1}}(s_1) - \tilde{\gamma}_{n+1}^{\sigma_{n+1}}(s_1)|_1 \leq \ \nu \ \ |\gamma_n^{\sigma_n}(s) - \tilde{\gamma}_n^{\sigma_n}(s)|_1, \quad 0 < \nu < 1.$$

It will be clear from the proof that this argument can be iterated to the desired estimate in $\mathcal{C}^3$. From the functional equation (6.5) and the fact that $|F_s| \geq \alpha > 1$ it follows that:

$$|\gamma_{n+1}^{\sigma_{n+1}}(s_1) - \tilde{\gamma}_{n+1}^{\sigma_{n+1}}(s_1)| \leq \ \max_{s\in\mathcal{I}_s, t\in\mathcal{I}_t}|G_t| \ |\gamma_n^{\sigma_n}(s) - \tilde{\gamma}_n^{\sigma_n}(s)|. \tag{6.7}$$

To estimate the derivative we use (6.6) and observe that it is of the form

$$\gamma_{n+1}^{\sigma_{n+1}}(s_1) = R(s, \gamma_n^{\sigma_n}(s)) + {\gamma^{\sigma_n}}' S(s, \gamma_n^{\sigma_n}(s)), \tag{6.8}$$

where the derivatives of R and S are small for ε small since $|F_s| \geq \alpha > 1$. Using this form, a mean value estimate gives

$$\begin{aligned} |{\gamma_{n+1}^{\sigma_{n+1}}}'(s_1) - {\tilde{\gamma}_{n+1}^{\sigma_{n+1}}}'(s_1)| &\leq c_1|\gamma_n^{\sigma_n}(s) - \tilde{\gamma}_n^{\sigma_n}(s)| + c_2|{\gamma_n^{\sigma_n}}'(s) - {\tilde{\gamma}_n^{\sigma_n}}'(s)|_1 \\ &\leq c_3|\gamma_n^{\sigma_n}(s) - \tilde{\gamma}_n^{\sigma_n}(s)|_1, \end{aligned} \tag{6.9}$$

for some constants c_1, c_2, c_3.

Using the estimates (6.7) and (6.9) we have that the map $\gamma_n^{\sigma_n}(s) \to \gamma_{n+1}^{\sigma_{n+1}}(s_1)$ is a contraction in $\mathcal{C}^1$. It then follows in a standard way that the iterates will converge to a unique solution of the functional equation (6.5). It can be seen from (6.8) that higher derivatives are estimated in the same way and we obtain a $\mathcal{C}^3$ invariant curve for the 2-D mapping. By construction this curve satisfies:

$$\mathcal{H}(s, \gamma(s)) \ = (F(s, \gamma(s)), \gamma \circ F(s, \gamma(s))).$$

This ends the proof of the Theorem (6.2). ∎

Using this invariant curve $\gamma(s)$, we have that the restricted dynamics is of the form

$$s \mapsto F(s) + \varepsilon^{2/3}\tilde{F}(s, \gamma(s)).$$

Since the perturbation is $\mathcal{C}^3$ one can compute the Schwartzian derivative which is clearly negative when ε is sufficiently small. This proves the existence of a chaotic motion in this class of model.

Moreover these orbits are confined in a exponentially small region around the orbit of the singular system. This does not preclude the existence of a more complicated invariant chaotic set. In fact the encoding of the intersection of these invariant curves with the t-axis, $t = \gamma_n^{\sigma_n}(s)$ provides a way to describe in detail the foliation of this unstable attractor. A complete study of this set is beyond the scope of this work and is the subject of a forthcoming paper.

References

[1] F.H Busse. K.E Heikes *Convection in a rotating layer: A simple case of turbulence.* Science, vol 208. (1980)

[2] P. Chossat, M. Krupa, I. Melbourne, A. Scheel, P. Chossat. *Transverse bifurcations of homoclinic cycles.* Physica D **100**, 85-100. (1997)

[3] B. Deng. *Spiral-Plus-Saddle attractors and elementary mechanisms for chaos generation.* Journal of Bifurcation and Chaos. Vol.6, No.**3**. pp 513-527. (1996)

[4] J. Guckenheimer. *Towards a global model theory of singularly perturbed dynamical systems.* Progress in Nonlinear Differential Equations and their applications, vol. **19**, 213-225. (1996)

[5] J. Guckenheimer, P. Holmes. *Structurally stable heteroclinic cycles.* Math. Proc. Camb. Phil. Soc. **103**, 189-192. (1988)

[6] M. Krupa, I. Melbourne. *Asymptotic Stability of Heteroclinic Cycles in systems with Symmmetry.* Erg.Th.Dyn.Sys. **15** 121-147. (1995)

[7] E.F Mischenko, Yu. S Kolesov, A. Yu Kolesov, N. Kh Rozov. *Asymptotic Methods in Singularly Perturbed Systems.* Monographs in Contemporary Mathematics. (1993)

[8] C. Robinson. *Dynamical systems; stability, symbolic dynamics and chaos.* CRC Press, Cleveland, OH. (1994)

[9] B. Sandstede, A. Scheel *Forced symmetry breaking of homoclinic cycles.* Nonlinearity **8**, 333-365. (1995)